Romanian Reports in Physics, Vol. 65, No. 2, P. 401–410, 2013

NUCLEAR PHYSICS

DISSIPATION FOR A WIDE MASS DISTRIBUTION IN FISSION, ALPHA-DECAY AND CLUSTER EMISSION

NAFISEH SHAYAN SHAKIB[1,a], MOHAMMAD FARHAD RAHIMI[2], MOHAMMAD MAHDI FIROOZABADI[1]

[1]Physics Faculty, University of Birjand,
P.O. Box 615/97175, Birjand, Iran
[2]Physics Faculty, Ferdowsi University of Mashhad, Azadi Square,
Post Code: 9177948974, Mashhad, Iran
E-mail[a]: nafiseh.shakib@gmail.com

Received September 20, 2012

Abstract. The dissipated energy in fission, cluster and alpha decay was estimated microscopically by using the time dependent pairing equations. The single particle level schemes were determined in the framework of the super asymmetric two centre shell model. A strong dependence of the dissipated energy as function of the mass asymmetry is evidenced. The dissipated energy is much lower for alpha decay and cluster emission than for fission.

Key words: Cluster emission, Alpha decay, Fission, time dependent pairing equations.

PACS: 25.85.Ca, 24.10.Eq, 21.30.Fe

1. INTRODUCTION

As mentioned earlier in Ref. [1], the motion of any real macroscopic physical system is not only managed by conservative forces. We need to take into account the dissipative forces that produce an irreversible flow of energy or angular momentum from the macroscopic degrees of freedom to the intrinsic ones. The concept of nuclear friction can be employed if we use collective coordinates and microscopic ones. A such ensemble can be found in the case when the Schrödinger equation is solved for microscopic potentials that vary in time. In nuclear physics, an interesting case could be that of nucleons that are moving in the Nilsson potential. This potential vary in time due to modifications of the generalized coordinates associated to the nuclear shape parametrization. In this context, by changing the generalized coordinates the fission process can be simulated.

In the following we will use the time dependent pairing equations [2–4] to de-

termine the dissipated energy for the fission, the alpha decay and ^{14}C emission of ^{236}U. The dissipated energy will be determined for predefined families of shapes that start from one spherical nucleus and ends as two separated fragments. A nuclear shape parametrization given by two intersected spheres of different radii will be used. Therefore, it is considered that the Nilsson two centre shell model [5,6] could be well describe the single particle energies needed to solve the time dependent pairing equations. The two centre model is a very power tool in solving two potentials in contact with a barest number of degrees of freedom. In this work, we will use only the two degrees of freedom associated to the elongation and to the mass asymmetry. Such calculations were realized in the past only for three fission channels [7] . We will investigate systematically the dissipated energy for all seniority zero fission partitions in the A-channels [8]. The results will be compared with the dissipation obtained for the alpha and carbon particles. As mentioned earlier in Ref. [1], the motion of any real macroscopic physical system is not only managed by conservative forces, but also by frictional ones. Therefore, in dynamical treatments we need to take into account the dissipative forces that produce an irreversible flow of energy or angular momentum from the macroscopic degrees of freedom to the intrinsic ones. The concept of nuclear friction can be employed if we use collective coordinates and microscopic ones. A such ensemble can be found in the case when the Schrödinger equation is solved for microscopic potentials that vary in time. In nuclear physics, an interesting case could be that of nucleons that are moving in the Nilsson potential.

2. THE MODEL

In our investigation, the time dependent pairing equations is used to evaluate the dissipation. The calculations are based on solutions given by the super asymmetric two centre shell model.

2.1. THE TWO CENTRE SHELL MODEL

Investigating the fission in a wide range of mass asymmetries, the two-centre shell models allow a continuous description of the changes of nuclear shapes from one initial nucleus to two final fragments. It is a generalization of the one centre Nilsson model. The two-centre shell-model Hamiltonian is obtained from the two-centre oscillator V_{2c} by adding the spin orbit interaction term V_{ls} and a correcting term V_{l^2} [9]. The Hamiltonian is:

$$H = T + V_{2c} + V_{ls} + V_{l^2}, \tag{1}$$

where T is the kinetic energy. The more general expression of the each terms valid at any deformation are

$$V_\rho = \frac{m\omega_\rho^2}{2}\rho^2 \tag{2}$$

$$V_z = \frac{m\omega_z^2}{2}\begin{cases}(z-z_1)^2 & , z>0;\\ (z+z_1)^2 & , z<0,\end{cases} \tag{3}$$

where the position of the two centres on the symmetry axis is given by $-z_1$ and $+z_1$. The spin orbit reads:

$$V_{ls} = -\chi\hbar\omega_0\{2\mathbf{s}(\bigtriangledown V\times\mathbf{p})+\mu[(\bigtriangledown V\times\mathbf{p})^2 - N(N+3)/2]\}, \tag{4}$$

where V is the two-centre oscillator potential. The Hamiltonian can be diagonalized in the basis of the two-centre symmetrical oscillator $|n_\perp\Lambda\nu_n s\pi>$.

The matrix elements of the operator V_{ls} are calculated in this basis by using the identities:

$$\mathbf{l}.\mathbf{s} = \frac{1}{2}(\mathbf{l}_+.\mathbf{s}_- + \mathbf{l}_-.\mathbf{s}_+) + \mathbf{l}_z.\mathbf{s}_z \tag{5}$$

$$l^2 = \frac{1}{2}(\mathbf{l}_+.\mathbf{l}_- + \mathbf{l}_-.\mathbf{l}_+) + l_z^2 \tag{6}$$

It must be mention that one has to replace z by $z-z_1$ when $z>0$, and $z+z_1$ when $z<0$, in order to obtain l_1 or l_2, respectively. The matrix elements: $< n'_\perp\Lambda'\nu'_n s'\pi' \mid H_0+V_{ls}\mid n_\perp\Lambda\nu_n s>$ are nonvanishing only if the states belong to the same subspace of the spin projection (Ω), where $\Omega=\Lambda+s$. The subspace $(-\Omega)$ can be obtained from (Ω) by changing Λ into $-\Lambda$ and s into $-s$. The Hamiltonian is diagonalized for positive and negative parities, separately by using numerical methods.

When the potential is separable in three dimensions, the condition

$$\left(\frac{\partial E}{\partial n_1}\right) : \left(\frac{\partial E}{\partial n_2}\right) : \left(\frac{\partial E}{\partial n_3}\right) = n_a : n_b : n_c \tag{7}$$

has to be fulfilled. Here n_a, n_b, n_c are small nonnegative integers and n_1, n_2, n_3 are quantum numbers.

For the spheroidal harmonic oscillator

$$E = \hbar\omega_z(n_z+\frac{1}{2}) + \hbar\omega_\perp(n_\perp+1) \tag{8}$$

$$E = \hbar\omega_0[(1-\frac{2}{3}\epsilon)(n_z+\frac{1}{2}) + (1+\frac{1}{3}\epsilon)(n_\perp+1)] \tag{9}$$

and the shell structure occurs when $\omega_\perp/\omega_z = (1+1/3\epsilon)(1-2/3\epsilon)^{-1} = n_c/n_a$; hence, $\epsilon = 3(n_c-n_a)/(n_a+2n_c)$. Several versions of super asymmetric two centre shell models used in fission are available in the literature, beginning with Nilsson potentials [10], Woods-Saxon ones [11–15], and terminating with relativistic ones [16].

2.2. DISSIPATED ENERGY

The microscopic description of the dynamics of a many nucleon system has been extensively investigated with the time dependent Hartree-Fork method [17]. However, in this method, the residual interactions are neglected. That leads to the unpleasant feature that a system even moving infinitely slowly could not end up in its ground state. In order to avoid all these difficulties one could use the pairing residual interaction. We shall start from the variational principle taking the following energy functional

$$\delta L = \delta < \varphi | H - i\hbar \frac{\partial}{\partial t} - \lambda N | \varphi >, \tag{10}$$

and we assume the many-body state as a BCS seniority zero wave function

$$|\varphi(t)>= \prod_{l} (u_l(t) + v_l(t) a_l^+ a_{\bar{l}}^+) |0> . \tag{11}$$

where $|0>$ denotes the vacuum state. a_l^+ and $a_{\bar{l}}^+$ are creation operators of the coupled states l and $\bar{l}$, and u_l and v_l are vacancy and occupation amplitudes, respectively and satisfy following relation

$$|v_l|^2 + |u_l|^2 = 1. \tag{12}$$

We know that only the relative phase between u_l and v_l matters, and decided to take u_l as a real quantity [3, 18].

Sometimes, this energy functional is called a Lagrangian. The functional contains several terms. The first one is the time dependent many-body Hamiltonian with pairing residual interactions

$$H(t) = \sum_{k>0} \epsilon_k(t) (a_k^+ a_k + a_{\bar{k}}^+ a_{\bar{k}}) - G \sum_{k,l>0} a_k^+ a_{\bar{k}}^+ a_l a_{\bar{l}}. \tag{13}$$

The particle number operator is

$$N = \sum_{k>0} (a_k^+ a_k + a_{\bar{k}}^+ a_{\bar{k}}). \tag{14}$$

By performing the variation of the Lagrangian in a way similar as in [11,18], the next system of coupled differential equations are obtained.

$$i\hbar \dot{\rho}_l = \kappa_l \Delta^* - \kappa_l^* \Delta, \tag{15}$$

$$i\hbar \dot{\kappa}_l = (2\rho_l - 1)\Delta + 2\kappa_l(\epsilon_l(t) - \lambda(t)) - 2G\rho_l\kappa_l, \tag{16}$$

where:

$$\Delta = G \sum_k \kappa_k, \tag{17}$$

$$\Delta^* = G \sum_k \kappa_k^*. \tag{18}$$

G is the pairing strength, Δ is the gap energy and

$$\kappa_k = u_k v_k, \tag{19}$$

$$\rho_k = |v_k|^2. \tag{20}$$

So, ρ_k are the single-particle densities and κ_k are the pairing moment components. ρ_k are real quantities, while κ_k are complex ones. In this context, the sum over pairs generally runs over index *k*. When the single-particle sum over *k* is realized only for one partner of each reversed pair, the result is multiplied by a factor 2. The index *k* runs over a workspace that allows the pairing force to operate only within a finite number of active levels around the Fermi energy.

The ground state energy E_0 of any deformation is obtained in the framework of the BCS formalism:

$$E_0 = 2\sum_k \rho_k^0 \epsilon_k - G\left|\sum_k \kappa_k^0\right|^2 - G\sum_k {\rho_k^0}^2 \tag{21}$$

in the static, lower energy state. Here, ρ_k^0 and κ_k^0 means solutions of the BCS equations. For the same deformation, the energy of an diabatic state m is obtained by considering the unpaired nucleon located on the diabatic state under consideration,

$$E' = 2\sum_k \rho_k \epsilon_k - G\left|\sum_k \kappa_k\right|^2 - G\sum_k \rho_k^2, \tag{22}$$

where the solutions of the TDHFB equations are used. In the frame of our model, the difference

$$\Delta E = E' - E_0 \tag{23}$$

behaves as a dissipation energy. Here E' is the energy of the system obtained within solutions of the time dependent pairing equations and E_0 is the BCS energy. These equations were recently used in the study of fission [19–21].

3. RESULTS

Three nuclear decay modes are treated in an unified manner. A nuclear shape parametrization given by two intersected spheres of different radii is used. We need to know the variation of the mass asymmetry as function of the elongation for each nuclear decay mode. Information about this dependence can be found in Refs. [22–24] where it was shown that in the case of very large mass asymmetries, that is, for alpha decay and cluster emission, the radius of the light fragment must be approximately constant $R_2 = 1.16 \times A_2^{1/3}$ fm. In the case of fission the light fragment emerges with a radius that gives approximately a constant emitted volume. A and A_2 denote

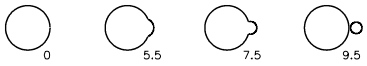

Fig. 1 – Family nuclear shapes, from the spherical configuration up to α emission. The distances between the center of the fragments in fm are marked on the plot.

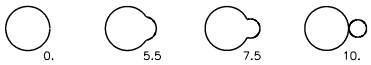

Fig. 2 – Same as Fig. 1 for the ^{14}C emission.

the mass numbers of the parent and of the light fission fragment, respectively. In the case of the alpha decay and of the ^{14}C emission, the shapes are displayed in Figs. 1 and 2, respectively. The emitted fragment starts to appear at an elongation $R = 1.16 \times ((A - A_2)^{1/3} - A_2^{1/3})$ fm. A different situation appears in the case of fission for which the shapes are plotted in Fig. 3. In this last case, a deviation from the spherical shape can be observed from the beginning of the process, that is $R \approx 0$. The neutron and proton level schemes are obtained with the superasymmetric two-center shell model improved in Ref. [6]. The fact that the nucleus begins to deforms at larger values of R is reflected by the variations of single particle levels schemes in the case of alpha decay and carbon emission as evidenced in Figs. 4 and 5. In the case of fission, a different situation appears, as displayed in Fig. 6. In the tree mentioned cases, the level scheme behave as a Nilsson diagram for prolate deformation. Having the level schemes for the three decay modes it is possible to compute

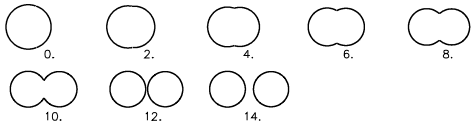

Fig. 3 – Same as Fig. 1 for fission.

the dissipation during the disintegrations with the time dependent pairing equations. The velocity of the internuclear distance was fixed at $\partial R/\partial t = 10^6$ m/s, that gives approximately 10^{-21} s as the time to tunnel the barrier [6]. This is considered as a characteristic time for scission.

Several A-channels were tested in the case of ^{236}U fission. We used the partitions that give a maximum fission yield as given by existing compilations [8]. In this context we simulated the even-even complementary fragments like: (^{120}Pd, ^{116}Pd), (^{118}Pd, ^{118}Pd), (^{116}Pd, ^{120}Pd), (^{114}Ru, ^{122}Cd), (^{112}Ru, ^{124}Cd), (^{110}Ru, ^{126}Cd), (^{108}Mo,

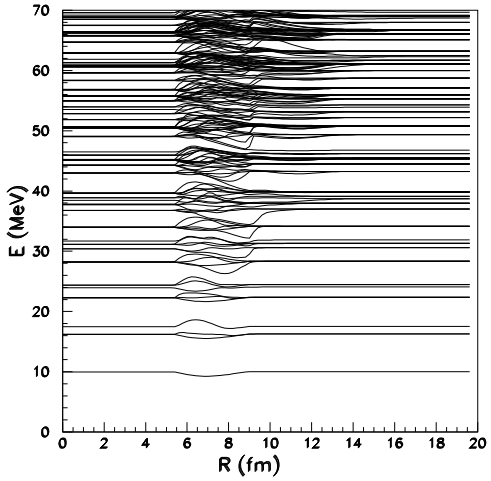

Fig. 4 – Neutron level scheme for α emission from ^{236}U.

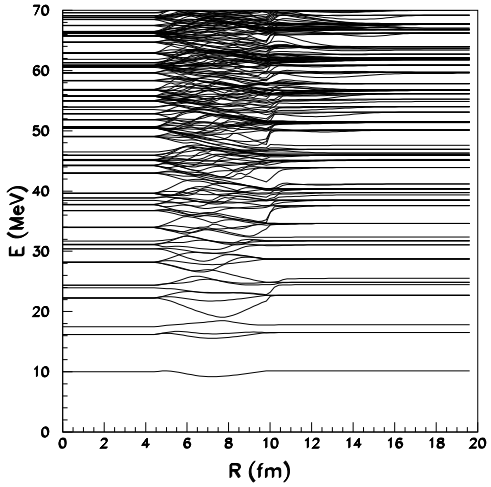

Fig. 5 – Neutron level scheme for ^{14}C emission from ^{236}U.

^{128}Sn), (^{106}Mo, ^{130}Sn), (^{104}Mo, ^{132}Sn), (^{102}Zr, ^{134}Te), (^{100}Zr, ^{136}Te), (^{98}Zr, ^{138}Te), (^{96}Sr, ^{140}Xe), (^{94}Sr, ^{142}Xe), (^{92}Kr, ^{144}Ba), (^{90}Kr, ^{146}Ba), (^{88}Kr, ^{148}Ba), (^{86}Se, ^{150}Ce), (^{84}Se, ^{152}Ce), (^{82}Ge, ^{154}Nd), (^{80}Ge, ^{156}Nd), and the last ones (^{78}Zn, ^{158}Sm).

In Fig. 7, the total dissipated energy in fission as function of the charge number A of the light fragment and the elongation R is represented. It is important to note that the dissipated energy at scission surpasses in general 7 MeV. For alpha decay and cluster emission, the dissipated energies as function of the elongation are represented

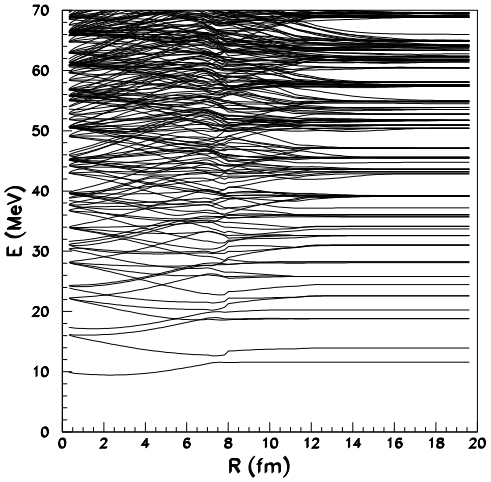

Fig. 6 – Neutron level scheme for the reaction $^{236}\mathrm{U} \longmapsto {}^{86}\mathrm{Se} + {}^{150}\mathrm{Ce}$

in Figs. 8 and 9. At scission the total dissipated energy amounts to 3 MeV for α decay and it is lower than 4.5 MeV for cluster emission. The dissipated energy reflect

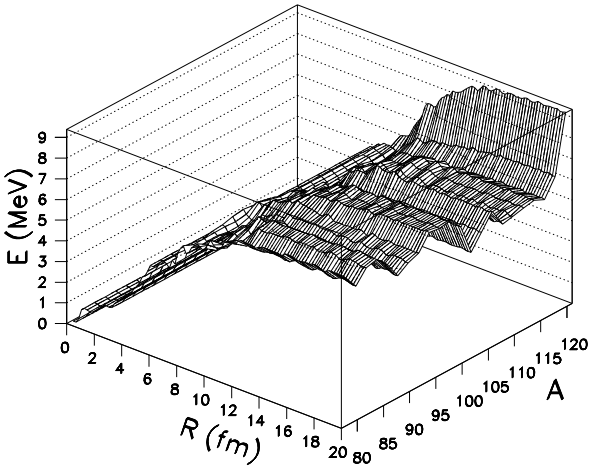

Fig. 7 – Dissipated energy as function of elongation R and the charge number A of the light fragment in fission.

differences in the structure of these three decay modes. The super asymmetric fission proceeds through adiabatic states, without dissipation, while in the fission at low energy a considerable amount of intrinsic excitation is produced. Therefore, the alpha decay and the cluster emission can be considered as cold rearrangement processes [25–28]. It is a confirmation of cold rearrangement hypothesis used in the prediction

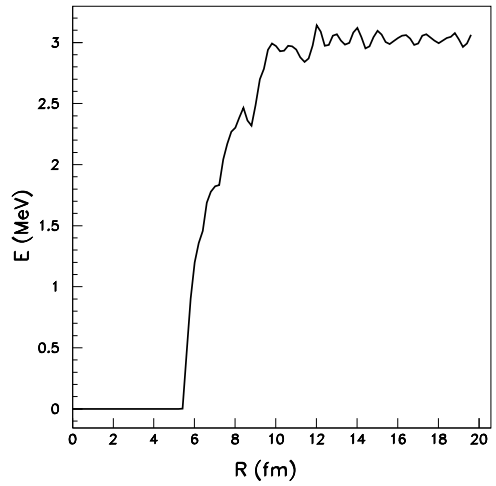

Fig. 8 – Dissipated energy as function of elongation in α-emission.

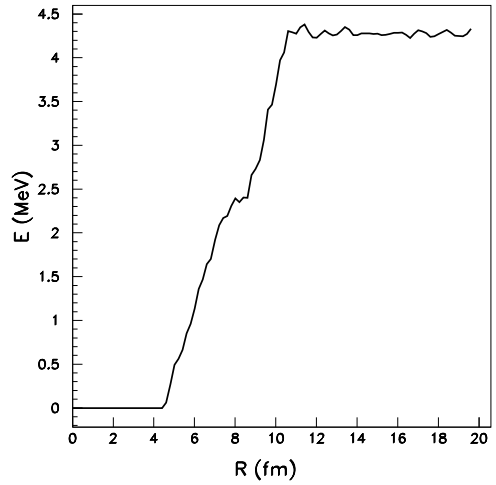

Fig. 9 – Dissipated energy as function of elongation in ^{14}C emission.

of cluster decay [29]. The differences in dissipated energy have their origin in the variations of the single particle energies. As observed in the level schemes, the degree of rearrangement of the levels is much lower for super asymmetric fission than for fission.

Our study treats the alpha decay within fission models as in Ref. [30]. In general this decay modes is analysed with preformation models [31, 32, 34, 35] or liquid

drop ones [36].

Acknowledgements. One of us (N.Sh.Sh.) wishes to express her love and gratitude to her beloved families especially her mother; for their understanding and endless love, through the duration of her studies. Also N. Sh. Sh. took benefit from a grant offered by the ministry of Science of Iran hosted by the Horia Hulubei National Institute of Physics and Nuclear Engineering - IFIN HH.

REFERENCES

1. R.W. Hasse, Rep. Progr. Phys. **41**, 1027 (1978).
2. S.E. Koonin and J.R. Nix, Phys. Rev. C **13**, 209 (1976).
3. J. Blocki and H. Flocard, Nucl. Phys. A **273**, 45 (1976).
4. G. Schutte and L. Wilets, Z. Phys. A **286**, 313 (1978).
5. M. Mirea, Phys. Rev. C **54**, 302 (1996).
6. M. Mirea, Phys. Rev. C **57**, 2484 (1998).
7. M. Mirea, L. Tassan-Got, C. Stephan and C.O. Bacri, Nucl. Phys. A **735**, 21 (2004).
8. A.C. Wahl, At. Data and Nucl. Data Tabl. **39**, 1 (1998).
9. D.N. Poenaru and M.S. Ivascu, *Particle Emission from Nuclei* (CRC Press) **1**, 113-173 (2000).
10. J. Maruhn and W. Greiner, Z. Phys. A **780**, 431 (1972).
11. M. Mirea, Phys. Rev. C **78**, 044618 (2008).
12. A. Diaz-Torres and W. Scheid, Nucl. Phys. A **757**, 373 (2005).
13. M. Mirea, Phys. Lett. B **680**, 316 (2009).
14. I. Companis, M. Mirea and A. Isbasescu, Rom. J. Phys. **56**, 63 (2011).
15. M. Mirea, Phys. Lett. B, doi:10.1016/j.physletb.2012.09.023.
16. L.-S. Geng, J. Meng and T. Hiroshi, Chin. Phys. Lett. **24**, 1865 (2007).
17. P.A.M. Dirac, Proc. Cambridge Phil. Roy. Soc. **26**, 376 (1930).
18. M. Mirea, Mod. Phys. Lett. A **18**, 1809 (2003).
19. B. Avez, C. Simenel and Ph. Chomaz, Phys. Rev. C **78**, 044318 (2008).
20. S. Ebata et al., Phys. Rev. C **82**, 034306 (2010).
21. M. Mirea, Int. J. Mod. Phys. E **21**, 1250035 (2012).
22. M. Mirea, D.N. Poenaru and W. Greiner, Z. Phys. A **349**, 39 (1994).
23. M. Mirea, D.N. Poenaru and W. Greiner, Nuovo Cimento A **105**, 571 (1992).
24. D.N. Poenaru, M. Mirea, W. Greiner, I. Cata and D. Mazilu, Mod. Phys. Lett. A **5**, 2101 (1990).
25. M. Mirea, A. Sandulescu and D.S. Delion, Eur. Phys. J. A **48**, 86 (2012).
26. M. Mirea, A. Sandulescu and D.S. Delion, Nucl. Phys. A **870-871**, 23 (2011).
27. M. Mirea, Rom. J. Phys. **57**, 372 (2012).
28. M. Mirea, A. Sandulescu and D.S. Delion, Proc. Rom. Acad. Series A **12**, 203 (2011).
29. A. Sandulescu and W. Greiner, J. Phys. G **3**, L189 (1977).
30. M. Mirea, Phys. Rev. C **63**, 034603 (2001).
31. I. Silisteanu, A.I. Budaca, Rom. J. Phys **57**, 493 (2012).
32. I. Silisteanu, A. Rizea, B.I. Ciobanu and A. Neacsu, Rom. J. Phys. **53**, 1191 (2008).
33. I. Silisteanu and A.I. Budaca, At. Data. Nucl. Data. Tabl. DOI: 10.1016/j.adt.2011.12.007.
34. D.S. Delion, A. Sandulescu, and W. Greiner, Phys. Rev. C **68**, 041303(R) (2003).
35. D.S. Delion, S. Peltonen, and J. Suhonen, Phys. Rev. C **73**, 014315 (2006).
36. V. Mirzaei and H. Miri-Hakimabad, Rom. Rep. Phys. **64**, 50 (2012).